Contemporary Mathematics

A Splitting Moving Mesh Method for 3-D Quenching and Blow-Up Problems

Kewei Liang and Ping Lin

Abstract. We present a splitting moving mesh method for multi-dimensional reaction-diffusion problems with nonlinear forcing terms over rectangular domains. The structure of the adaptive algorithm is an elegant combination of an operator splitting and one-dimensional moving mesh. It is motivated by the nature of splitting method, which splits a multi-dimensional problems into a few one-dimensional problems. Therefore, the temporal and the spatial adaptations are adopted based on one-dimensional arc-length equidistributed rule. The method not only keeps the advantage of splitting methods on reducing computational cost but also simplifies the implementation of moving mesh techniques. The method is first presented in [**20**] for the 2-D quenching problems using Peaceman-Rachford splitting. In this paper, we apply the splitting moving mesh method to both the 3-D blow-up and the 3-D quenching singularity using Douglas splitting. 3-D numerical examples will be given to demonstrate the good performance of the method.

1. Introduction

Many important physical phenomena, such as metastability, phase transition, oscillations and finite time blow-up, can be modeled by a multi-dimensional reaction-diffusion equation

$$\frac{\partial u}{\partial t} = \nabla \cdot (A\nabla u) + f(u, \nabla u, x, t), \tag{1.1}$$

where ∇ is the gradient operator, $x \in \mathbb{R}^m$, $\nabla \cdot (A\nabla u)$ is the diffusion term and f is a given function representing nonlinear reactive sources. Here the solution u, often representing the dimensionless temperature, has dynamic singularities and nonuniformities for some choices of $f(u, \nabla u, x, t)$. We will consider two cases. In one case f is a polynomial or exponential function of u such that $f \to \infty$ as $u \to \infty$, for example $f = u^3$. This application arises in population dynamics, linear beam theory, plasma physics, chemical reactor theory and the combustion theory [**3, 21, 22**]. The main interest is a possibility that the solution may tend

1991 *Mathematics Subject Classification.* 65K20, 65M50, 35K65, 35B40.

Key words and phrases. nonlinear reaction-diffusion equations, blow-up, quenching singularity, Douglas splitting, moving mesh method.

The work was supported in part by Singapore Academic Research Grant under No. R-146-000-053-112.

to infinity in a finite time. This phenomenon is called *blow-up*. In the other case we have the reaction term that satisfies $f \to \infty$ as $u \to 1$ (or a finite number), for example $f(u) = \dfrac{1}{(1-u)^\theta}$, $\theta > 0$. This type of reaction-diffusion equation with singular reaction term arises in the study of quenching phenomena and electric current transients in polarized ionic conductors. In this case the solution is bounded, while its derivative with respect to time blows up in a finite time. We will call this phenomenon as *quenching or extinction*. It is also significant in the theory of ecology and environmental studies, especially in the prediction and control of pipeline decays [**9, 18, 22, 23**].

From a computational point of view, it is well known that the use of uniform fixed mesh can not resolve such strong singularity of solution efficiently, since the solution develops in relatively small time intervals or spatial length scales. It is essential to use some adaptive numerical methods with both temporal and spatial adaptations for computing such singular behavior. The strategy of proper finite difference schemes with moving mesh techniques has been widely used in one-dimensional quenching singularity and the blow-up simulations [**3, 23**]. Studies of efficient adaptive finite difference method for multi-dimensional problems require much more effort [**5, 9, 15, 19, 20**]. The key difficulty is that the high dimension causes tremendous increases in the amount of computations and the complexity of adaptation. However, splitting techniques offer efficient and effective ways to convert higher dimensional problems into a set of lower dimensional equations and at the same time offer easy parallelization to largely reduce computational time. It also seems to us that such a splitting can be done relatively easier by using the finite difference method. This motivates our splitting moving mesh method which is an elegant combination of splitting and moving mesh. Since splitting adaptation is always done in a one-dimensional setting, various one-dimensional adaptive techniques can be applied easily and successfully. Moreover, due to the splitting nature, the splitting moving mesh method not only keeps the advantage of reducing computational cost but also is simple and easy to implement.

For stating clearly and simply, we will only consider the following nonlinear reaction-diffusion problem in three-dimensional case.

$$u_t = \alpha u_{xx} + \beta u_{yy} + \gamma u_{zz} + f(u),\ (x,y,z,t) \in \Omega, \tag{1.2}$$

$$u(x,y,z,t) = b(x,y,z,t),\ (x,y,z,t) \in \Gamma, \tag{1.3}$$

$$u(x,y,z,0) = u_0(x,y,z),\ (x,y,z) \in \mathcal{D}, \tag{1.4}$$

where $\alpha,\ \beta,\ \gamma$ are functions of (x,y,z), $\mathcal{D} = (0,1)\times(0,1)\times(0,1)$, with its boundary $\partial\mathcal{D}$ and $\Omega = \mathcal{D} \times (0,\ T)$, $\Gamma = \partial\mathcal{D} \times (0,\ T)$ with $0 < T < \infty$. Generalization to more dimensions is straightforward. The splitting method and splitting moving mesh method have been first studied in [**9, 20**] with stability and monotonicity analysis for a two-dimensional quenching model. In this paper, we will discuss its implementation issues for general three-dimensional problems. We will consider both blow-up and quenching solutions of (1.2)-(1.4).

The paper is organized as follows. In §2, a 3-D Douglas splitting scheme is presented. We will then introduce the moving mesh methods in both temporal and spatial directions and summarize our algorithm in §3. The applications of the splitting moving mesh method in §4 focus on the 3-D blow-up and 3-D quenching singularity. The numerical results demonstrate that the method is very efficient for these problems with point singularities.

2. The splitting scheme for reaction-diffusion problems

In [**9, 20**], we show that Peaceman-Rachford splitting method is efficient and accurate for solving nonlinear reaction-diffusion problems in two-dimensional quenching problems. The split systems of equations developed with nonsingular tridiagonal coefficient matrices are numerically stable. But for 3-D cases Douglas splitting method is still better in both stability and accuracy [**11, 12**]. Thus we adopt Douglas splitting method for problem (1.2)-(1.4) with explicit treatment of the nonlinear reaction term.

We introduce a mesh on the spatial domain $\overline{\mathcal{D}} = \mathcal{D} \cup \partial\mathcal{D}$ with grid points (x_i, y_j, z_k), $0 \le i \le I+1$, $0 \le j \le J+1$, $0 \le k \le K+1$ and a partition in time

$$\{0 = t_0 < t_1 < \cdots < t_n < \cdots < T\}. \tag{2.1}$$

Let $u^n_{i,j,k}$ be an approximation of the solution at the grid point (x_i, y_j, z_k, t_n), $i = 0, 1, \dots, I+1$, $j = 0, 1, \dots, J+1$, $k = 0, 1, \dots, K+1$ and $n = 0, 1, \cdots$. We replace the spatial derivatives $u_{xx}(x_i, y_j, z_k, t_n)$, $u_{yy}(x_i, y_j, z_k, t_n)$ and $u_{zz}(x_i, y_j, z_k, t_n)$ respectively by finite differences

$$\delta^2_x u^n_{i,j,k} \equiv \alpha_{i,j,k}\left(u(x_i, y_j, z_k, t_n)\right)_{\bar{x}\hat{x}} = \frac{\alpha_{i,j,k}}{\hbar_{x,i}}\left[\frac{u^n_{i+1,j,k} - u^n_{i,j,k}}{h_{x,i}} - \frac{u^n_{i,j,k} - u^n_{i-1,j,k}}{h_{x,i-1}}\right],$$
$$\delta^2_y u^n_{i,j,k} \equiv \beta_{i,j,k}\left(u(x_i, y_j, z_k, t_n)\right)_{\bar{y}\hat{y}} = \frac{\beta_{i,j,k}}{\hbar_{y,j}}\left[\frac{u^n_{i,j+1,k} - u^n_{i,j,k}}{h_{y,j}} - \frac{u^n_{i,j,k} - u^n_{i,j-1,k}}{h_{y,j-1}}\right]$$

and

$$\delta^2_z u^n_{i,j,k} \equiv \gamma_{i,j,k}\left(u(x_i, y_j, z_k)\right)_{\bar{z}\hat{z}} = \frac{\gamma_{i,j,k}}{\hbar_{z,k}}\left[\frac{u^n_{i,j,k+1} - u^n_{i,j,k}}{h_{z,k}} - \frac{u^n_{i,j,k} - u^n_{i,j,k-1}}{h_{z,k-1}}\right]$$

with $\alpha_{i,j,k} = \alpha(x_i, y_j, z_k)$, $\beta_{i,j,k} = \beta(x_i, y_j, z_k)$, $\gamma_{i,j,k} = \gamma(x_i, y_j, z_k)$, $h_{x,i} = x_{i+1} - x_i$, $h_{y,j} = y_{j+1} - y_j$, $h_{z,k} = z_{k+1} - zk$, $\hbar_{x,i} = (h_{x,i} + h_{x,i-1})/2$, $\hbar_{y,j} = (h_{y,j} + h_{y,j-1})/2$, $\hbar_{z,k} = (h_{z,k} + h_{z,k-1})/2$ and $i = 0, 1, \dots, I+1$, $j = 0, 1, \dots, J+1$, $k = 0, 1, \dots, K+1$, $n = 1, 2, \cdots$. Further, we denote

$$U_n = (u^n_{1,1,1}, u^n_{2,1,1}, \dots, u^n_{I,1,1}, \dots, u^n_{I,J,1}, u^n_{1,1,2}, \dots, u^n_{I,J,K})^T$$

and

$$g(U_n) = \left(f(u^n_{1,1,1}), f(u^n_{2,1,1}), \dots, f(u^n_{I,J,1}), f(u^n_{1,1,2}), \dots, f(u^n_{I,J,K})\right)^T.$$

Then Douglas splitting method (plus an explicit treatment of the nonlinear term) can be written as

$$U_{n+\frac{1}{3}} = U_n + \tau_n\left[\delta^2_x \overline{U}_{n+\frac{1}{3}} + \left(\delta^2_y + \delta^2_z\right)U_n + g\left(\frac{w_n + U_n}{2}\right)\right], \tag{2.2}$$

$$U_{n+\frac{2}{3}} = U_n + \tau_n\left[\delta^2_x \overline{U}_{n+\frac{1}{3}} + \delta^2_y \overline{U}_{n+\frac{2}{3}} + \delta^2_z U_n + g\left(\frac{w_n + U_n}{2}\right)\right], \tag{2.3}$$

$$U_{n+1} = U_n + \tau_n\left[\delta^2_x \overline{U}_{n+\frac{1}{3}} + \delta^2_y \overline{U}_{n+\frac{2}{3}} + \delta^2_z \overline{U}_{n+1} + g\left(\frac{w_n + U_n}{2}\right)\right], \tag{2.4}$$

where

$$w_n = U_n + \tau_n\left[\left(\delta^2_x + \delta^2_y + \delta^2_z\right)U_n + g(U_n)\right], \tag{2.5}$$

$\overline{U}_{n+i} = \dfrac{U_{n+i} + U_n}{2}$, $i \in \{1/3, 2/3, 1\}$ and $\tau_n = t_{n+1} - t_n$, $n = 0, 1 \cdots$.

REMARK 2.1. *In the 3-D case, the Douglas splitting scheme with above nonlinear treatment (2.2)-(2.4) has the second order accuracy in both time and space, if the mesh is uniform (noting that the Peaceman-Rachford splitting scheme is only of order one in time)* [**11**]. *Moreover, the scheme is equivalent to the Peaceman-Rachford splitting method presented in* [**9, 20**] *in the 2-D case.*

3. Splitting moving mesh method and numerical implementation

The splitting algorithm in previous section provides an efficient way for the multi-dimensional computation and significant amount of operations can be saved. However, since the strong singularity in solution causes rapid variations in both temporal and spatial directions, numerical methods using a uniform mesh are difficult to reproduce such singular behavior. Moving mesh method has had success in resolving such singularity, where mesh points are concentrated locally in the regions with rapid variations in solution during the solution process [**3, 4, 10, 14**]. It has been demonstrated that significant improvements in accuracy and efficiency can be achieved by moving mesh method. Especially, moving mesh technique is generally well understood for one-dimensional problems. But the challenges of moving mesh method still remain for multi-dimensional problems. This motivates our splitting moving mesh method which is a combination of splitting method and moving mesh method [**20**]. We now consider the 3-D case.

3.1. Temporal adaptation. We introduce the following arc-length monitor function

$$m(u, t) = \sqrt{1 + \left(\frac{\partial \mu(u, u_t)}{\partial t}\right)^2}, \tag{3.1}$$

where the choice function μ is dependent of the solution behavior of PDE problem. For example, we can select $\mu(u, u_t) = u_t$ for quenching type problem and $\mu(u, u_t) = u$ for blow-up type problem.

Following the temporal discretization (2.1), we require the arc-lengths in the temporal neighboring intervals $[t_{n-2}, t_{n-1}]$ and $[t_{n-1}, t_n]$ be equivalent. Then, from (3.1), the temporal step size τ_n can be determined by

$$\tau_n^2 = \tau_n^2 + ((\mu)_{n-1} - (\mu)_{n-2})^2 - ((\mu)_n - (\mu)_{n-1})^2, \; n = 2, 3, \cdots, \tag{3.2}$$

where τ_0 and τ_1 are given [**9, 20**].

REMARK 3.1. *The adaptation may have problems, when the solution is near the strong singularity. So we choose a minimal temporal step size controller $\tau_{\min}$, $0 < \tau_{\min} << \tau_0$, to avoid sudden changes in grid movement or any unnecessarily large number of computations near the singularity* [**9**]. ∎

3.2. Moving mesh method in space. In spatial directions we shall use the equidistribution principle to produce efficient computational meshes. We have no need to design a sophisticated multi-dimensional equidistribution principle since our splitting method splits a multi-dimensional problem to a number of one-dimensional problems. Our goal is to use a monitor function working for general problems. So we use the conventional one-dimensional equidistribution principle. Certainly, if we known more information about the solution of the problem, we may construct better monitor function (see a test example in Remark 3.2 and [**7**]). We follow the notation in [**20**] and use the following one-dimensional equidistribution principle:

$$\int_{x_i}^{x_{i+1}} m(u,x)\,dx = \frac{1}{I+1}\int_{x_0}^{x_{I+1}} m(u,x)\,dx, \tag{3.3}$$

$$\int_{y_j}^{y_{j+1}} m(u,y)\,dy = \frac{1}{J+1}\int_{y_0}^{y_{J+1}} m(u,y)\,dy, \tag{3.4}$$

$$\int_{z_k}^{z_{k+1}} m(u,z)\,dz = \frac{1}{K+1}\int_{z_0}^{z_{K+1}} m(u,z)\,dz, \tag{3.5}$$

$$m(u,s) = \sqrt{1+\left(\frac{\partial\mu(u,u_t)}{\partial s}\right)^2} \tag{3.6}$$

where s may be spatial variable x, y or z, function μ may be the same as one in Subsection 3.1. In (3.3), (3.4) and (3.5), x_i, y_j and z_k are nonuniform mesh points in x, y and z directions, respectively. For example, we consider the mesh redistribution in x-direction when $t = t_n$. First, we fix y and z. On each line $y = y_j,\ z = z_k$ there are grid points $(x_0^{(y_j,z_k)}, y_j, z_k), (x_1^{(y_j,z_k)}, y_j, z_k), \cdots, (x_{I+1}^{(y_j,z_k)}, y_j, z_k)$. Starting from the boundary point $(x_0^{(y_j,z_k)}, y_j, z_k)$ we can easily determine $x_1^{(y_j,z_k)}, \ldots, x_I^{(y_j,z_k)}$ using above formula (3.3). We adopt a finite difference approximation for $\left.\dfrac{\partial\mu(u,u_t)}{\partial s}\right|_{y=y_j,z=z_k,t=t_n}$ and a numerical integration formula (based on the piecewise linear approximation of $m(u,s)$). Then we get the new x-coordinates of all grid points along each line $y = y_j,\ z = z_k,\ j = 1,\cdots,J,\ k = 1,\cdots,K$. Since $x_i^{(y_j,z_k)}$ may be not the same for fixed i and different j,k. We can hence take a new i-th x-coordinate x_i^{new} by the following way:

$$x_i^{new} = x_i^{y_{\hat{j}},k_{\hat{k}}}, \text{ where } \hat{j}, \text{ and } \hat{k} \text{ are indices such that}$$
$$\left|\frac{\partial\mu(u,u_t)}{\partial x}\right|_{x=x_i,y=y_{\hat{j}},z=z_{\hat{k}},t=t_n} = \max_{j,k}\left|\frac{\partial\mu(u,u_t)}{\partial x}\right|_{x=x_i,t=t_n}.$$

By far, we get a set of new grid points (x_i^{new}, y_j, z_k), $i = 1,\cdots,I, j = 1,\cdots,J, k = 1,\cdots,K$. Similarly, the new j-th y-coordinate $y_j^{new} = y_j^{x_{\hat{i}},z_{\hat{k}}}$ and the new k-th z-coordinate $z_k^{new} = z_k^{x_{\hat{i}},y_{\hat{j}}}$ can be determined by (3.4) and (3.5) respectively. So we get the finial new grid points $(x_i^{new}, y_j^{new}, z_k^{new})$ before marching to the next time step t_{n+1}.

REMARK 3.2. *Indeed, if we know more priori information of the singularities of the solution, we may construct a monitor function to achieve the second order convergence (e.g. in* [**7**] *authors constructed a second order convergence of a monitor function due to the preestimated information of the singularly perturbation solution). Unfortunately, for blow-up and quenching problems, the theoretical analysis about the high order spatial derivative of the solution is not available. Nevertheless, there is a conjecture about the solution behavior (quenching rate) near the quenching which is also verified in our numerical computation. We may construct the time arc-length monitor function by the conjectured quenching or blow-up rate function (see* [**16**]*), which is* $\mu(u,u_t) = (T_h - t)^{1/[2(\theta-1)]}$*, where* T_h *is the numerical blow-up time and* θ *is the exponent in the nonlinear force* $f(u) = u^\theta$ *(*$\theta = 3$ *for the first example in Subsection 4.1). Keeping the arc-length monitor function in space,* *we indeed get the same blow-up time* $T_h^* = 0.006224$ *if we let* $T_h = 0.006224$ *in* $\mu(u, u_t) = (T_h - t)^{1/(2\times 2)}$. *While, if we choose other* $T_h^{'} \neq 0.006224$ *in* $\mu(u, u_t)$, *we cannot get the same blow-up time* $T_h^{'}$. *For example, we choose* $T_h = 0.006229$ *in* $\mu(u, u_t)$ *and we can not get* $T_h^* = 0.006229$. *This may also serve as a justification of the quenching or blow-up time as well.*

3.3. Interpolation. As mentioned in the previous subsection, we adjust (move) the spatial mesh according to the spatial monitor function at the time step t_n before marching to the next time step t_{n+1}. We thus have to use $\tilde{u}_n$, which is the solution defined on the new mesh, as the initial condition of the splitting numerical method. $\tilde{u}_n$ can be approximated by polynomial interpolation:

$$\tilde{u}_n = I_p u_n,$$

where I_p is a matrix associated with a tri-p-th order polynomial interpolation. For computational accuracy, we use the tri-quadratic interpolation I_2 ($p = 2$). Assuming that (X_i, Y_j, Z_k) is a grid point of new mesh and its position lies, for example, in a box $[x_{i-1}, x_{i+1}] \times [y_{j-1}, y_{j+1}] \times [z_{k-1}, z_{k+1}]$, we have

$$\begin{aligned}
& \tilde{u}(X_i, Y_j, Z_k) \\
= \; & (1-\gamma_1-\gamma_2)\tilde{u}(X_i, Y_j, z_{k-1}) + \gamma_1 \tilde{u}(X_i, Y_j, z_k) + \gamma_2 \tilde{u}(X_i, Y_j, z_{k+1}) \\
= \; & (1-\gamma_1-\gamma_2)\Big[(1-\beta_1-\beta_2)\tilde{u}(X_i, y_{j-1}, z_{k-1}) + \beta_1 \tilde{u}(X_i, y_j, z_{k-1}) \\
& \quad + \beta_2 \tilde{u}(X_i, y_{j+1}, z_{k-1})\Big] \\
& + \gamma_1 \Big[(1-\beta_1-\beta_2)\tilde{u}(X_i, y_{j-1}, z_k) + \beta_1 \tilde{u}(X_i, y_j, z_k) + \beta_2 \tilde{u}(X_i, y_{j+1}, z_k)\Big] \\
& + \gamma_2 \Big[(1-\beta_1-\beta_2)\tilde{u}(X_i, y_{j-1}, z_{k+1}) + \beta_1 \tilde{u}(X_i, y_j, z_{k+1}) + \beta_2 \tilde{u}(X_i, y_{j+1}, z_{k+1})\Big],
\end{aligned}$$

where

$$\tilde{u}(X_i, \cdot, \cdot) = (1-\alpha_1-\alpha_2)u(x_{i-1}, \cdot, \cdot) + \alpha_1 u(x_i, \cdot, \cdot) + \alpha_2 u(x_{i+1}, \cdot, \cdot),$$

and

$$\begin{aligned}
\alpha_1 &= \frac{(X_i - x_{i-1})(x_{i+1} - X_i)}{h_{x,i-1}h_{x,i}}, \quad \alpha_2 = \frac{(X_i - x_{i-1})(X_i - x_i)}{(h_{x,i-1} + h_{x,i})h_{x,i}}, \\
\beta_1 &= \frac{(Y_j - y_{j-1})(y_{j+1} - Y_j)}{h_{y,j-1}h_{y,j}}, \quad \beta_2 = \frac{(Y_j - y_{j-1})(Y_j - y_j)}{(h_{y,j-1} + h_{y,j})h_{y,j}}, \\
\gamma_1 &= \frac{(Z_k - z_{k-1})(z_{k+1} - Z_k)}{h_{z,k-1}h_{z,k}}, \quad \gamma_2 = \frac{(Z_k - z_{k-1})(Z_k - z_k)}{(h_{z,k-1} + h_{z,k})h_{z,k}}.
\end{aligned}$$

3.4. Numerical procedure. Let us summarize the above exposition by enumerating the numerical procedures for the splitting moving mesh method.

(1) Initialize data:
  (a) Construct the initial spatial mesh: the uniform mesh $h_x = h_{x,i}$, $h_y = h_{y,j}$, $h_z = h_{z,k}$, $x_{i+1} = x_i + h_x$, $y_{j+1} = y_j + h_y$, $z_{k+1} = z_k + h_z$, $i = 0, \cdots, I$, $j = 0, \cdots, J$, $k = 0, \cdots, K$;
  (b) Give the initial temporal step size τ_0;
  (c) Compute U_0 based on the initial condition $u_0(x, y, z)$;
(2) Advance the solution to next steps:
  (i) Evolve the solution U_n with the temporal step size τ_n based on appropriate splitting scheme, such as (2.2)-(2.4) in section 2;

(ii) Repeat (i) for the desired number (say $l-1$) of time steps ($\tau_n = \tau_{n+1} = \cdots = \tau_{n+l-1}$).

(3) Calculate a new temporal step size τ_{n+l} followed by (3.2) in Subsection 3.1.
(4) Implement moving mesh method in space direction according to (3.3), (3.4) and (3.5).
(5) Interpolate to obtain the approximation solution $\tilde{U}_{n+l}$ on the new spatial mesh (still denoted as U_{n+l}).
(6) repeat (2)-(5) with new temporal step size τ_{n+l}, new spatial mesh and U_{n+l} until the stopping criteria is met.

REMARK 3.3. *In the above algorithm, the main procedures of (2) and (4) can be easily parallelized. As the presentation in subsection 3.2, the one-dimensional adaptation is done at each line $x = x_i$ $(1 \le i \le I)$, $y = y_j$ $(1 \le j \le J)$ or $z = z_k$ $(1 \le k \le K)$. The computation at one grid line is independent of that at other grid lines and thus can be done simultaneously by assigning it to multi-processors. Similarly, the stages (2.2)-(2.4) are involved with a number of one-dimensional implementation and can also be parallelized (cf.* [**20**] *for 2-D examples).*

4. Applications

We consider two kinds of $f(u)$ in problems (1.2)-(1.4), as mentioned in Introduction, whose solution develops the blow-up or quenching singularity respectively. These are good examples to test adaptive numerical techniques as shown in [**8, 9**] for the 2D cases. In this section, we will first apply our splitting moving mesh method in two-dimensional blow-up type problem in order to compare the result with those in [**5, 8**]. Then we apply our method to three-dimensional cases. The numerical results shows again that our method can efficiently follow the high variation of three-dimensional solutions and successfully capture the point singularity behavior of the solution.

4.1. Blow-up singularity. We first discuss nonlinear reaction-diffusion problems with the blow-up solution. A special 2-D case studied in [**8**] is

$$u_t = u_{xx} + u_{yy} + f(u), \ (x,y) \in \mathcal{D}, \ 0 < t < T, \tag{4.1}$$

$$u(0,y,t) = u(a,y,t) = u(x,0,t) = u(x,b,t) = 0, \ 0 < t < T; \tag{4.2}$$

$$u(x,y,0) = u_0(x,y), \ (x,y) \in \mathcal{D}. \tag{4.3}$$

where $f(u)$ is a polynomial function of u such that $\dfrac{f(u)}{u} \to \infty$ as $u \to \infty$. This problem represents an explosive instability of the process due to the effect of the nonlinear terms [**2, 17**]. It is well known that if u_0 is sufficiently large there is a blow-up time $T < \infty$ such that

$$\lim_{t \to T^-} \sup_{(x,y) \in \mathcal{D}} |u(x,y,t)| = \infty, \tag{4.4}$$

i.e., the solution blows up [**3**].

Let $f(u) = u^3$, $u_0(x,y) = 10\sin(\pi x)\sin(\pi y)$ and $\mathcal{D} = (0,1) \times (0,1)$ in (4.1). We use $N = 41 \times 41$ grid points. Figure 4.1 shows the solution u and the spacial mesh immediately before the blow-up at $t = 0.006224$. Note that when $t = 0.006224$, $\max_{(x,y)\in\mathcal{D}} u = 1.4337 \times 10^{16}$. We take $t = 0.006224$ as an approximation of the blow-up

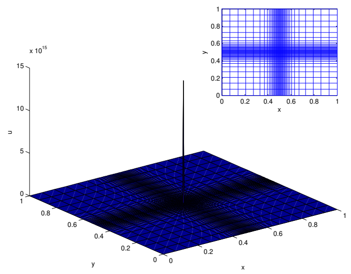

FIGURE 4.1. *The solution u and the spatial mesh immediately before the blow-up at $t = 0.006224$ ($f(u) = u^3, u_0 = 10\sin(\pi x)\sin(\pi y), \tau_0 = 1.0 \times 10^{-6}$ and $\tau_{\min} = 1.0 \times 10^{-10}$). The peak of u in main graph has reached 1.4337×10^{16}. The spatial mesh is plotted as a sub-graph.*

time, which is slightly smaller than $t = 0.00629$ obtained in [**8**] (where 120×120 grid points are used).

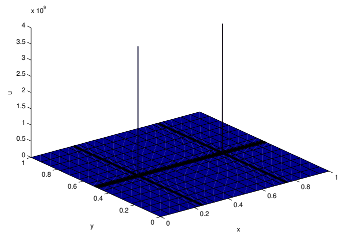

FIGURE 4.2. *The solution u immediately before the blow-up at $t = 0.002463$ ($f(u) = 4\sqrt{1+u^5}, u_0 = 20\sin^2(2\pi x)\sin^2(\pi y), \tau_0 = 1.0 \times 10^{-6}$ and $\tau_{\min} = 1.0 \times 10^{-10}$). The top value of u has reached 3.99×10^9.*

We next choose $f(u) = 4\sqrt{1+u^5}$ and $u_0(x,y) = 20\sin^2(2\pi x)\sin^2(\pi y)$. It is noted that two humps lie along the x-direction in initial solution u_0 and evolve rapidly into two peaks. Figure 4.2 presents the numerical solution with two peaks at $t = 0.002463$. This blow-up time is a little smaller than the times $t = 0.00258$ and $t = 0.00249$ (128×128 grid points are used) reported respectively in [**5, 8**]. A more detailed graph about the spatial mesh and a close-up look of the part $[0.24, 0.26] \times [0.48, 0.52]$ near the left peak are displayed in Figure 4.3. We note that the left peak exactly lies at the point $(2.5, 0.5)$ where it should be and does not has the phenomenon of slight shift in [**5, 8**] (see Fig. 5 of [**5**]).

We extend the blow-up type problem to the three-dimensional case.

$$u_t = u_{xx} + u_{yy} + u_{zz} + f(u), \ (x,y,z) \in \mathcal{D}, \ 0 < t < T, \tag{4.5}$$

$$u(x,y,z,t) = 0, \ (x,y,z,t) \in \Gamma; \tag{4.6}$$

$$u(x,y,z,0) = u_0(x,y,z), \ (x,y,z) \in \mathcal{D}. \tag{4.7}$$

where $\mathcal{D} = (0,1) \times (0,1) \times (0,1)$ and $\Gamma = \partial\mathcal{D} \times (0,T)$.

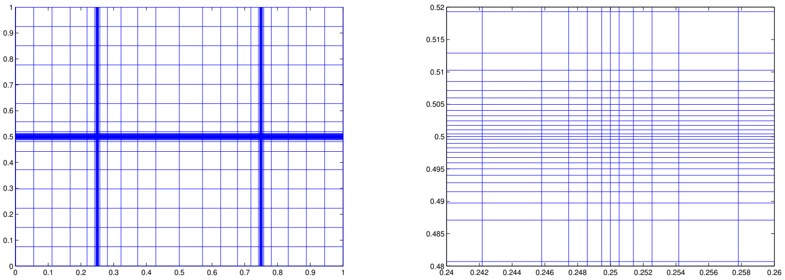

FIGURE 4.3. *The spatial meshes immediately before the blow-up at* $t = 0.002463$ *(*$f(u) = 4\sqrt{1+u^5}, u_0 = 20\sin^2(2\pi x)\sin^2(\pi y), \tau_0 = 1.0\times 10^{-6}$ *and* $\tau_{\min} = 1.0\times 10^{-10}$*). LEFT: The profile of the whole spatial mesh is displayed. RIGHT: The range* $[0.24, 0.26]\times[0.48, 0.52]$ *of the left graph is enlarged. And the left peak exactly lies at the point* $(0.25, 0.5)$.

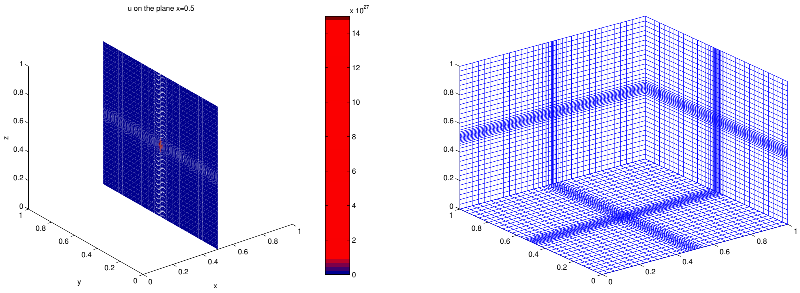

FIGURE 4.4. *The solution* u *and the spatial mesh of the 3-D blow-up problem immediately before the blow-up (*$f(u) = u^3, u_0 = 10\sin(\pi x)\sin(\pi y)sin(\pi z), \tau_0 = 1.0\times 10^{-6}$ *and* $\tau_{\min} = 1.0\times 10^{-8}$*). LEFT: The solution* u *is displayed when* $t = 0.007249$*. The location of the maximal solution* $u = 1.4984\times 10^{28}$ *is the center point* $(0.5, 0.5, 0.5)$ *at the plane* $x = 0.5$*. RIGHT: The projections in the planes* $x = 1$*,* $y = 1$ *and* $z = 0$ *of the adaptive spatial mesh.*

We will adopt $N = 41\times 41\times 41$ discretization grid points in space for all 3-D case examples. We test the case of $f(u) = u^3$ with the initial condition $u_0 = 10\sin(\pi x)\sin(\pi y)sin(\pi z)$. Figure 4.4 depicts the solution u and the spatial mesh immediately before the blow-up at $t = 0.007249$. At this time, the location of the maximal solution $u = 1.4984\times 10^{28}$ is the center point $(0.5, 0.5, 0.5)$ at the plane $x = 0.5$.

Similarly as the 2-D problem, we further consider the case of two singular points. Let $f(u) = 4\sqrt{1+u^5}$ and $u_0 = 20\sin^2(2\pi x)\sin^2(\pi y)\sin^2(\pi z)$. There are two singular points along the x-direction as shown in the left graph of Figure 4.5. In the right graph of Figure 4.5 we draw three contour plane $x = 0.25$, $x = 0.75$ and $z = 0.5$ to show clearly the locations of two singular points. It can be observed that the locations of two singular points are the centers of two upright contour planes, i.e., $(0.25, 0.5, 0.5)$ and $(0.75, 0.5, 0.5)$ respectively. And the maximal solution is $u = 1.5850 \times 10^{10}$.

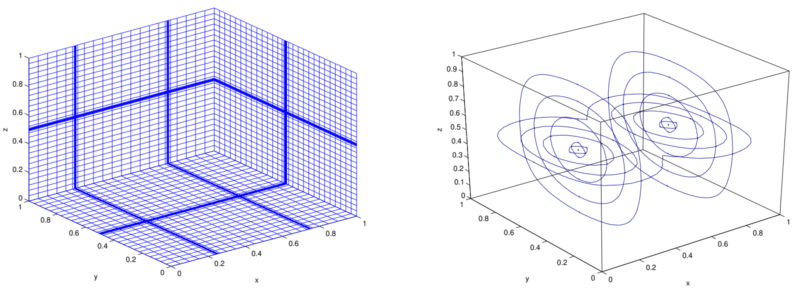

FIGURE 4.5. *The spatial adaptive mesh and the contour planes of the 3-D blow-up problem immediately before the blow-up at* $t = 0.001748$ *(*$f(u) = 4\sqrt{1+u^5}, u_0 = 20\sin^2(2\pi x)\sin^2(\pi y)\sin^2(\pi z), \tau_0 = 1.0 \times 10^{-6}$ *and* $\tau_{\min} = 1.0 \times 10^{-8}$*). The locations of two singularity points are* $(0.25, 0.5, 0.5)$ *and* $(0.75, 0.5, 0.5)$ *respectively. LEFT: The projections in the planes* $x = 1$*,* $y = 1$ *and* $z = 0$ *of the adaptive spatial mesh is given. RIGHT: Three contour planes* $x = 0.25$*,* $x = 0.75$ *and* $z = 0.5$ *are plotted. The maximal solution is* $u = 1.5850 \times 10^{10}$.

4.2. Quenching singularity. The quenching problem in three-dimensional case without degeneracy can be formulated as

$$u_t = \alpha u_{xx} + \beta u_{yy} + \gamma u_{zz} + \frac{1}{(1-u)^{\theta}}, \ 0 < t < T, \tag{4.8}$$

$$u(x, y, z, t) = 0 \ (x, y, z, t) \in \Gamma; \tag{4.9}$$

$$u(x, y, z, 0) = 0, \ (x, y, z) \in \mathcal{D}. \tag{4.10}$$

where α, β and γ are constants and $\theta > 0$.

In some specific applications (See [**1**]), u represents the temperature in the combustion channel, x and y are coordinates perpendicular and parallel to the channel walls, respectively. The initial temperature $u_0 \geq 0$ and is usually very small (it is thus usually assumed to be zero). The solution u of (4.8)-(4.10) is said to *quench* if there exists a finite time T such that

$$\sup\left\{|u_t(x, y, z, t)| : (x, y, z) \in \bar{\mathcal{D}}\right\} \to \infty \text{ as } t \to T^-.$$

The value T is then defined as the *quenching time* [**1, 18**]. A necessary condition for quenching to occur is

$$\max\left\{|u(x, y, z, t)| : (x, y, z) \in \bar{\mathcal{D}}\right\} \to 1^- \text{ as } t \to T^-. \tag{4.11}$$

Figure 4.6 gives the solution u and its first time derivative u_t immediately before quenching at $t = 0.796940$ in three-dimensional case. We use the colors to show the different values of u and u_t. In the right graph of Figure 4.6, the derivative u_t has the maximal value 252.3817 at the center point $(2.5, 2.5, 2.5)$. Similarly, the solution u gets its maximum at the center point of the plane $x = 2.5$ in the left graph. Further, since the adaptive mesh is symmetric with respect to $x = 2.5$, $y = 2.5$ and $z = 2.5$ respectively, the part $(0 \leq x \leq 2.5, 0 \leq y \leq 2.5, 2.5 \leq z \leq 5)$ of

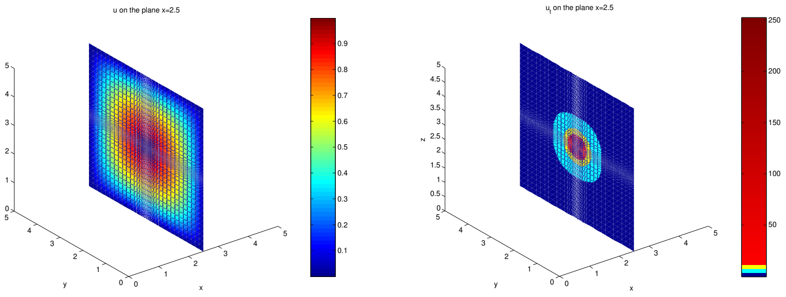

FIGURE 4.6. *The function* u *and its time derivative* u_t *on plane* $x = 2.5$ *immediately before quenching at* $t = 0.796940$ *in three-dimensional case* ($\alpha = \beta = \gamma = 1/25$, $\theta = 1$, $\tau_0 = 0.001$ *and* $\tau_{\min} = 1.0 \times 10^{-5}$). *LEFT: We note that the solution* u *gets its maximum at the center point* $(2.5, 2.5, 2.5)$ *of the plane* $x = 2.5$. *RIGHT: The derivative* u_t *has also the maximal value* 252.3817 *at the center point* $(2.5, 2.5, 2.5)$ *of the plane* $x = 2.5$.

the three-dimensional space is shown in Figure 4.7. The projections in the planes $x = 2.5$, $y = 2.5$ and $z = 2.5$ of the adaptive mesh are displayed in Figure 4.7. It is observed that the mesh is also refined in a small local region of the center point $(2.5, 2.5, 2.5)$.

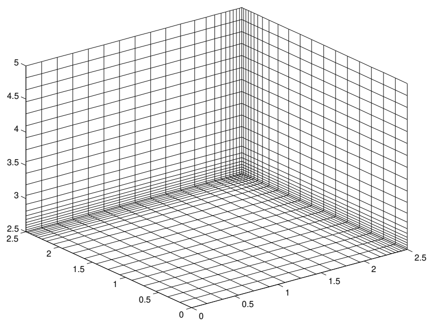

FIGURE 4.7. *The projections in the planes* $x = 2.5$, $y = 2.5$ *and* $z = 2.5$ *of the adaptive mesh of the problem (4.8)-(4.10).*

In [**20**] we verified a conjecture about the quenching rate in two-dimensional quenching problem. Here we similarly consider the quenching rate based on the numerical results for the three-dimensional case. We take the evolution of $\ln(1 - u(2.5, 2.5, 2.5, t))$ as a function of $\ln(T - t)$, where point $(2.5, 2.5, 2.5)$ is the quenching point and T is the quenching time. The slope of the obtained curve approximately gives the quenching rate (conjectured as $1/(1 + \theta)$ in 2-D case). The slope in the left profile of Figure 4.8 is $1/2$ when the problem (4.8)-(4.10) with $\theta = 1$ is considered. Similarly, the slope in the right is $1/4$ when $\theta = 3$. Furthermore, we may estimate the constant of the quenching rate at the quenching point, that is, $(1 - u) = 1.0774(T - t)^{1/2}$ and $(1 - u) = 1.2743(T - t)^{1/4}$ for the case of $\theta = 1$ and

$\theta = 3$ respectively. These results show that the conjecture about quenching rate $1/(1+\theta)$ in the 2-D case may also hold for the 3-D case.

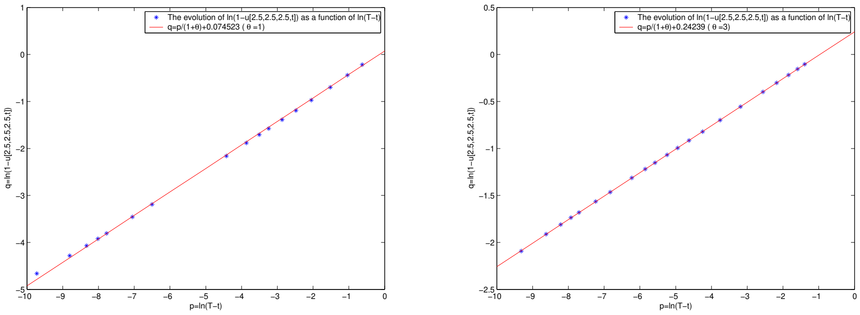

FIGURE 4.8. *The quenching rate for three-dimensional quenching problems* ($\alpha = \beta = \gamma = \dfrac{1}{25}$)*. The slope of the curve measures the quenching rate. And the line connecting the points is obtained by the least square approximation. LEFT:* $\theta = 1$ *and* $(1-u) = 1.0774(T-t)^{1/2}$*; RIGHT:* $\theta = 3$ *and* $(1-u) = 1.2743(T-t)^{1/4}$.

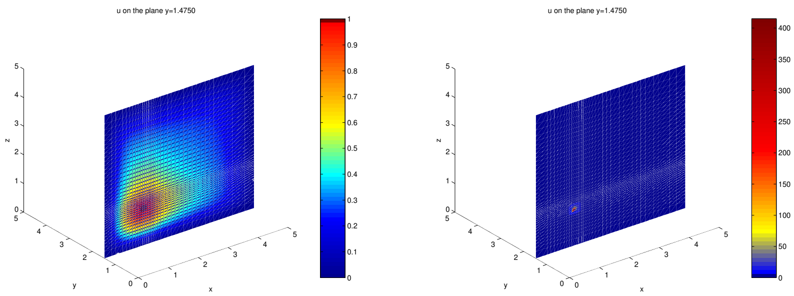

FIGURE 4.9. *The solution* u *and its derivative* u_t *of the problem in subsection 4.3 immediately before quenching* ($q = 1$, $L = 5.0$, $\theta = 1$, $\tau_0 = 0.001$ *and* $\tau_{\min} = 1.0 \times 10^{-4}$)*. LEFT: The solution* u *is displayed in the left graph when* $t = 1.6157$*. It is noted that the solution* u *gets its maximum at the point* $(1.4750, 1.4750, 1.4750)$ *of the plane* $y = 1.4750$*. RIGHT: The derivative* u_t *has also the maximal value* 414.7637 *at the point* $(1.4750, 1.4750, 1.4750)$ *of the plane* $y = 1.4750$.

4.3. Degenerate quenching singularity . Consider the case of $\alpha = \beta = \gamma = L^{-(q+2)}\left(x^2+y^2+z^2\right)^{-q/2}$, $(L > 0,\ q > 0)$ and $f(u) = L^{-q}\left(x^2+y^2+z^2\right)^{-q/2}(1-u)^{-\theta}$, in (1.2). The function $\alpha(x,y,z)$, $\beta(x,y,z)$ or $\gamma(x,y,z)$ represents certain singularity in the temperature transportation speed which causes the degeneracy in the differential equation (1.2) (See [**6, 13**] for more details). Figure 4.9 depicts a slice of the solution u and its derivative u_t immediately before quenching in the case of $q = 1$. Since the effect of the coefficient $(x^2+y^2+z^2)^{-q/2}$, the location of quenching point shifts slightly from the center to $(1.4750, 1.4750, 1.4750)$. This shift of quenching point towards the origin point (0,0,0) well agrees with the similar predictions in two-dimensional case in [**9**].

In summary, from Figure 4.3 and 4.7, we note the fact that the spatial refinement has been restricted to a small area of the whole domain where the solution develops singularity when t approaches a finite time. This indicates the efficiency of the splitting moving mesh method for the problems with point singularity patterns.

Acknowledgement

We thank Tang Tao for bringing us to attention of the reference [**8**] and valuable discussion.

References

1. A. Acker and B. Kawohl, *Remarks on quenching*, Nonlinear Anal. **13** (1989), 53–61.
2. J. Bebernes and D. Eberly, *Mathematical problems from combustion theory*, Springer-Verlag, New York, 1989.
3. C. J. Budd, W. Huang, and R. D. Russell, *Moving mesh methods for problems with blow-up*, SIAM J. Sci. Comput. **17** (1996), 305–327.
4. W. Cao, W. Huang, and R. D. Russell, *A moving mesh method in multiblock domains with application to a combustion problem*, Numer. Methods Partial Diff. Eqns. **15** (1999), 449–467.
5. H. Ceniceros and T. Hou, *An efficient dynamically adaptive mesh for potentially singular solutions*, J. Comp. Phys. **172** (2001), 609–639.
6. C. Y. Chan and P. C. Kong, *Channel flow of a viscous fluid in the boundary layer*, Quart. Appl. Math. **55** (1997), 51–56.
7. Long Chen and Jinchao Xu, *Qusi optimality of the streamline diffusion finite element of the one-dimensional singularly perturbed problem*, Accepted by AMS Contemporary Mathematics Series: Recent Advances in Adaptive Computation, Hangzhou, 2004.
8. Shaohua Chen, Robert D. Russell, and Wentao Sun, *Comparison of some moving mesh methods in higher dimensions*, Manuscript.
9. H. Cheng, P. Lin, Q. Sheng, and R.C.E. Tan, *Solving degenerate reaction-diffusion equations via variable step Peaceman-Rachford splitting*, SIAM J. Sci. Comput. **25** (2003), 1273–1292.
10. J. M. Coyle, J.E. Flaherty, and R. Ludwig, *On the stability of mesh equidistribution strategies for time-dependent partial differential equations*, J. Comput. Phys. **62** (1986), 26–39.
11. J. Douglas, *Alternating direction methods for three space variables*, Numer. Math. **4** (1962), 41–63.
12. J. Douglas and J. E. Gunn, *A general formulation of alternating direction methods I. Parabolic and hyperbolic problems*, Numer. Math. **6** (1964), 428–253.
13. M. S. Floater, *Blow-up at the boundary for degenerate semilinear parabolic equations*, Arch. Rational Mech. Anal. **114** (1991), 57–77.
14. R. M. Furzeland, J. G. Verwer, and P. A. Zegeling, *A numerical study of three moving-grid methods for one-dimensional partial differential equations which are based on the method of lines*, J. Comput. Phys. **89** (1990), 349–388.
15. W. Huang and R. D. Russell, *Moving mesh strategy based on a gradient flow equation for two-dimensional problems*, SIAM J. Sci. Comput. **20** (1999), no. 3, 998–1015.
16. Motos Júla and Souplet Philippe, *Universal blow-up rates for a semilinear heat equation and applications*, Advances in Differential Equations **8** (2003), no. 5, 615–639.
17. A. A. Lacey, *The form of blow-up for nonlinear parabolic equations*, Proc. Roy. Soc. Edinburgh **98A** (1984), 183–202.
18. H. A. Levine, *Quenching, nonquenching, and beyond quenching for solutions of some parabolic equations*, Ann. Math. Pure. Appl. **4** (1989), 243–260.
19. R. Li, T. Tang, and P. Zhang, *Moving mesh methods in multiple dimensions based on harmonic maps*, J. Comp. Phys. **170** (2001), 562–588.
20. K.W. Liang, P. Lin, M.T. Ong, and R.C.E. Tan, *A splitting moving mesh method for reaction-diffusion equations of quenching type*, Tech. Report 791, Department of Mathematics, National University of Singapore, 2004.

21. C.V. Pao, *Nonlinear parabolic and elliptic equations*, Plenum Press, New York, 1992.
22. Timo Salin, *Quenching and blowup problems for reaction diffusion equations*, Ph.D. thesis, Helsinki University of Technology, Institute of Mathematics Research Reports, Helsinki University of Technology, 2004.
23. Q. Sheng, *A monotonically convergent adaptive method for nonlinear combustion problems*, Integral Methods in Science & Engineering, (Research Notes in Math., 418), Chapman & Hall/CRC, London and New York, 2000, pp. 310–315.

Department of Mathematics, National University of Singapore, 2 science drive 2, Singapore 117543.
E-mail address: matlkw@nus.edu.sg

Department of Mathematics, National University of Singapore, 2 science drive 2, Singapore 117543.
E-mail address: matlinp@nus.edu.sg